

## COLLIMATION SYSTEM FOR THE BESSY FEL\*

T. Kamps

Berliner Elektronenspeicherring-Gesellschaft für Synchrotronstrahlung  
BESSY, D-12489 Berlin, Germany

### Abstract

Beam collimation is an essential element for the successful running of a linear accelerator based free electron laser. The task of the collimation system is to protect the undulator modules against mis-steered beam and dark-current. This is achieved by a set of apertures limiting the succeeding transverse phase space volume and magnetic dogleg structure for the longitudinal phase space. In the following the design of the BESSY FEL collimation system is described together with detailed simulation studies.

### MOTIVATION

Experiences from linac driven FEL operation (for example at TTF1 [1]) indicate that beam collimation is essential in order to provide protection of the undulator modules ensuring safe FEL operation.

The collimator section serves as transverse and longitudinal phase space filter which lets particles within a certain energy bandwidth and transverse phase space volume pass. Particles outside this region are blocked and cannot be lost in the undulator modules. In the transverse plane this is achieved by a set of apertures limiting the succeeding transverse phase space volume. In addition the collimator is designed to remove halo and dark-current created and transported through the linac upstream. The various halo sources include the bunch compressor, wakefield generated tails in the linac, mis-matched and mis-steered beam, and particles produced by Coulomb Scattering. In the longitudinal plane off-energy particles are dark current electrons and energy tails produced in the bunch compressors. Dark current is mainly created in the gun and through field emission in the super-conducting cavities [2]. Another important role for the collimator is set during the commissioning of the machine as linac and collimator tune-up dumps are part of the system.

### Undulator Protection

The BESSY FEL facility [3] will provide light from three different lines running at different energies. Each FEL line will have its own collimator section directly in front of the undulator modules. The collimator is designed with the high energy beamline running at 2.3 GeV electron beam energy in mind but is without any modifications adaptable for all other FEL lines. The modulators and radiators of the FEL are realized as planar pure permanent

magnet undulators. Each undulator is composed of modules with length ranging from 1.6 m to 3.9 m, the total length of the high energy FEL line is 70 m. A FODO lattice is superimposed onto the undulator structure with the quadrupole magnets located at the intersections between the undulator modules. For the present analysis in total 14 undulator modules are taken into account for the simulation studies. The gap between the undulator poles is 10 mm, the beampipe radius is 4 mm. The undulator magnets are made of NdFeB in order to obtain large undulator K parameters. This material is very sensitive to irradiation, especially to the reduced dose deposited by high-energy electrons (> 20 MeV). From studies with NdFeB under electron irradiation [4] the limit for acceptable beam loss in the undulator chamber has been derived. It can be shown that for 1% demagnetization the acceptable beam loss in the vacuum chamber is 300 nC [3]. It is evident that a collimator system together with a fast-acting machine protection system must be included in the FEL design.

### Machine Protection System

The three FEL lines will initially operate at a bunch repetition frequency of 1 kHz each. With a bunch charge of 2.5 nC and a beam energy of  $\leq 2.3$  GeV the beam power is  $3 \times 6$  kW. At no location in the accelerator the structures can withstand the power load for 6 successive incidents, the vacuum chamber wall will be destroyed within 2 ms. The goal of the machine protection system will be to limit the relative beam loss to  $10^{-5}$  of the maximum beam current. This can be achieved by comparing the signals of a series of fast current monitors that allow one to measure the bunch charge at a precision of better than 0.2 pC. Together with two other systems based on NaI beam loss monitors and optical fibers this safety chain of triple redundancy will be able to enable machine operation in case of sudden beam losses.

## SYSTEM OVERVIEW

In Fig. 1 the general layout of the collimator section is depicted. After the last accelerating module the beam enters first the transverse collimation section containing a matching quadrupole triplet and the two transverse collimator apertures. From there the beam passes another matching section before going through a dogleg structure made up with two dipole magnets separated by a drift region with a quadrupole triplet. The two energy collimators are located before the first and after the third quadrupole.

\* Funded by the Bundesministerium für Bildung und Forschung, the state of Berlin and the Zukunftsfonds Berlin

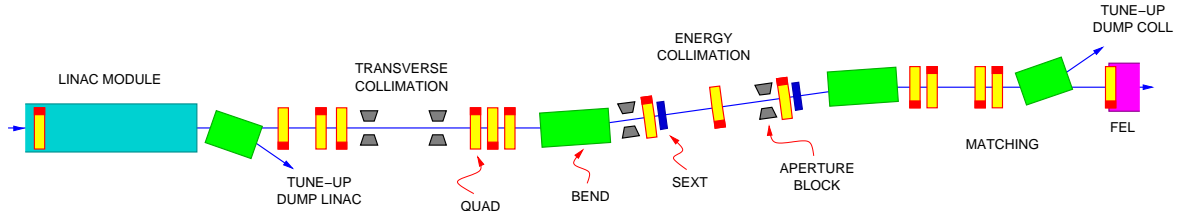


Figure 1: Collimator beamline including the last accelerating module and the beginning of the FEL undulator section.

An additional set of sextupoles is placed close to these quadrupoles. In order to minimize the flux of photons escaping the transverse collimation section the dogleg is placed between undulator and transverse collimation section. The collimator beamline ends with the last matching section preparing the twiss parameters according to the specification of the undulator lattice. The section contains two tune-up dump beam exits. One directly after the linac, the other just before the entrance of the undulator. The whole section is less than 43 m long.

### Transverse Collimation

For transverse collimation many configurations with aperture slots or holes are possible [5]. The most common solution is to place a thin ( $\sim 1/2$  radiation length) spoiler with a small aperture in front of a long ( $\sim 20$  radiation length) absorber block with a slightly larger aperture. The spoiler produces a large transverse momentum spread in the intercepted particles. The increased transverse momentum spread is converted into a large radial spread which is completely attenuated by the following absorber block. Two or more pairs are located in an optics channel with adequate twiss functions, which could be a FODO lattice with  $\pi/2$  phase advance between two pairs.

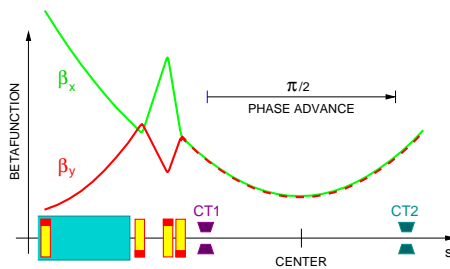


Figure 2: Transverse collimation scheme with two apertures CT1 and CT2.

In order to keep the BESSY FEL collimator system as compact as possible and the total length under 50 m the scheme with two spoiler-absorber pairs was dropped in favor of a setup with two single absorbers. Recent studies for the TTF2 collimator [6] show that with this scheme a high collimation efficiency can be achieved with just two apertures working in parallel for both transverse dimensions. The transverse collimation section contains two absorber

blocks separated by  $\pi/2$  phase advance. Each block is fitted with a small round aperture limiting the passage for the horizontal and vertical direction at the same position. This scheme requires that the twiss parameters for both dimensions are the same as well as the phase advance. This is achieved by producing a waist with the beam coming from the linac by means of a quadrupole triplet as shown in Fig. 2. The beam enters the transverse collimator from left coming out of the last accelerating section. The quadrupole triplet focuses the beam in both dimension to waist, which is located at the center between the two apertures CT1 and CT2. The horizontal phase space portrait at the center between CT1 and CT2 is illustrated in Fig. 3. The inner

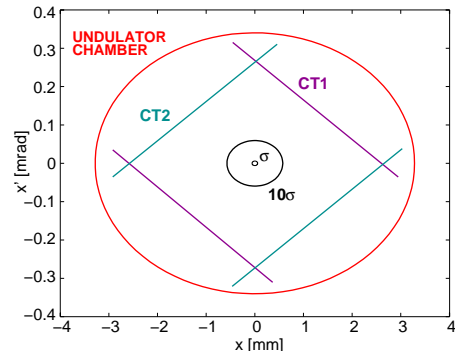


Figure 3: Phase space portrait at the center between CT1 and CT2. Also shown is the inner boundary of the back-transformed undulator vacuum chamber.

boundary of the undulator vacuum chamber is completely shaded by the two apertures. The area inside the parallelogram is the upper limit for the collimator acceptance and is given by the beam stay clear distance  $\Delta x_{clear}$  and the maximum beta function in the undulator  $\beta_{max}$  according to

$$a_{coll} \leq \frac{(r_{pipe} - \Delta x_{clear})^2}{2\beta_{max}} \quad (1)$$

and for the given case the collimator acceptance is  $a_{coll} = 0.3575 \mu\text{m}$ . From this the aperture radius can be calculated with  $g_{coll} = \sqrt{a_{coll} \cdot L_{coll}}$  where the transverse collimator length  $L_{coll}$  is the distance between the two apertures CT1 and CT2 which is equal to the value for the betafunction at this location. The collimator aperture radius is then 2.6 mm. In the following copper is assumed for the absorber material. More studies are underway to compare the

performance for copper and titanium. The length of the absorber is around 10 radiation length and thus 140 mm. In order to minimize wakefield effects and to keep the total block length within limits a step-in plus taper combination was chosen for the transition between gap radius to beam pipe radius. At the step-in the aperture changes from 20 mm beam pipe radius to 5 mm at the taper start. The taper length is 200 mm bringing the radius down to the value of 2.6 mm as required at the aperture. The exit face of the collimator block is of the same design. Taper radius and length have been chosen to minimize the transverse wakefield kick on the beam. The same type of absorber blocks are also used in the energy collimation section.

### Energy Collimation

Energy collimation is achieved with apertures in a closed dispersion bump created by a magnetic dogleg structure. The scheme is depicted in Fig. 4. The optics consists of

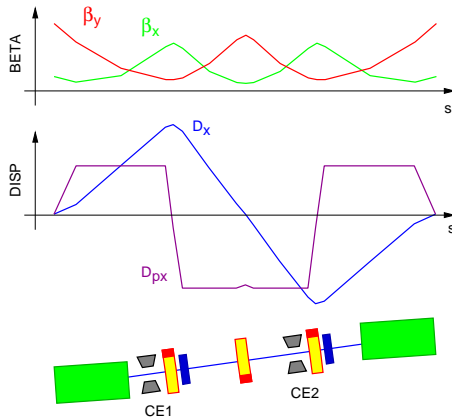


Figure 4: Energy collimation scheme with dogleg bend and two apertures CE1 and CE2.

two bending magnets with  $2.5^\circ$  bending angle separated by  $2\pi$  phase advance. The phase advance is realized over the short length of the dogleg of roughly 9 m by a three quadrupoles. Sextupoles are added at locations of high dispersion to reduce orbit deviations at the undulator entrance for off-energy particles. The apertures are also located at points where the electrons are mainly sorted according to their energy deviation close to the outer two quadrupoles. The first aperture CE1 has a slightly larger radius of 3.75 mm providing an energy cut at  $\pm 10\%$  for dark-current rejection. The second aperture is of the same kind as the apertures in the transverse collimation part. With a local dispersion function of around 0.1 m the acceptance bandwidth is around 5% energy spread. The total length of the dogleg is 8.8 m producing an orbit offset of 0.36 m.

### SIMULATION STUDIES

The twiss parameters in the collimator beamline are plotted in Fig. 5 together with the locations of the various aper-

tures.

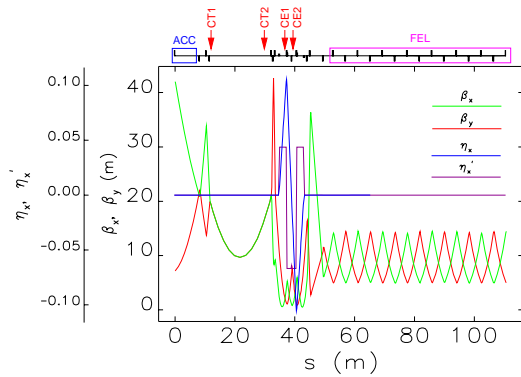


Figure 5: Twiss parameters in the collimator and undulator sections.

Particle losses and the energy bandwidth of the collimator system have been simulated using the elegant simulation package [7]. In Fig. 6 results for a seed with  $5 \times 10^5$  particles filling the whole beam pipe with an emittance of 5250 mm mrad with an energy spread of  $dp/p = 0.10$ . The plots in Fig. 6 show the loss distribution along the beamline and phase space portraits at the end of the undulator beamline. The energy bandwidth of the system is  $\pm 4.7\%$ . From these simulations it can be concluded that no primary particle can hit the inner vacuum chamber of the undulator beam pipe. The sextupole magnets inside the dogleg keep the orbit deviation for off-energy particles down. Switching these magnets off results in orbit deviation of up to 1 mm for electrons with 5% energy deviation.

Back-reaction on the electron beam in terms of wakefields and coherent synchrotron radiation (CSR) effects have been estimated. The emittance growth due CSR effects in the bending magnets leads to an emittance growth of 0.1% for the vertical and 2% for the horizontal emittance for an input emittance of 1.5 mm mrad and energy spread of 0.01%. The taper angle was chosen such that the resistive and geometric wakefield kicks are equal [8]. This results with a bunch length of  $\sigma_t = 1$  ps and gap radius of 2.6 mm to a taper angle of roughly 75 mrad. After the local radius has reached 5 mm a step-in realizes the transition to the nominal beam pipe radius.

### Diagnostics

The collimator section is a key component in the linac beamline as it is positioned directly in front of the FEL undulator. All phase space parameters like emittance, bunch length and energy spread can be measured here. For orbit steering some quadrupoles in the beamline will be equipped with stripline BPMs. For tuning of the transverse collimator an OTR station is planned for the location of the beam waist between CT1 and CT2. The energy spread can be measured with another OTR station in the dispersive arm. To study the efficiency of the dark cur-

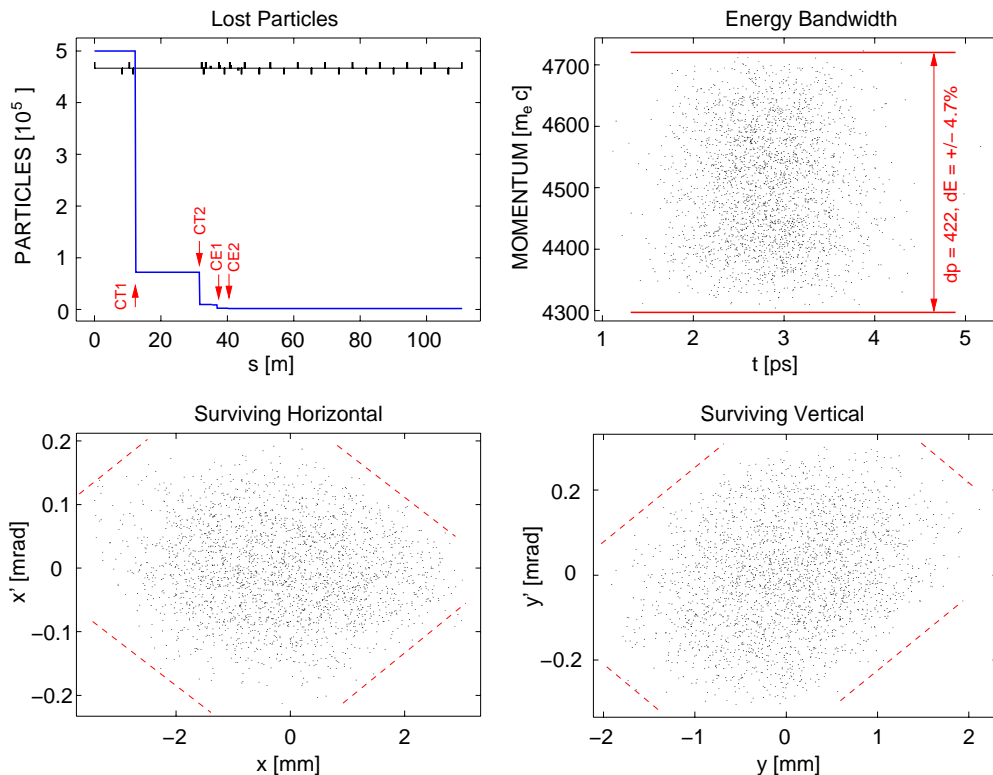


Figure 6: Performance studies for particle losses. Top left: Particle losses along the beamline. Top right: Final energy bandwidth of the particle distribution. Bottom left and right: Horizontal and vertical phase space at the undulator exit.

rent suppression current transformers are located in front of and after the dogleg. Besides that more current transformers will be put at the beginning and the end of the collimator section to monitor overall transmission through the system. The dipole chambers will all have exit windows to enable detection of the synchrotron radiation for beam profile measurements. For commissioning the collimator section is equipped with two tune-up dumps, one straight after the linac enabling commissioning of the linac without the need to bring the beam through the collimator. The other tune-up dump is located just in front of the first FEL undulator module.

## CONCLUSION AND OUTLOOK

A collimator system for the BESSY FEL has been discussed. The system is compact and protects the undulator against impact by off-momentum and mis-steered particles. With the next steps damage limits for the collimator material have to be derived. Furthermore the performance for secondary particles will be studied.

## ACKNOWLEDGMENTS

The author would like to thank M. Abo-Bakr, N. Golubeva and M. Körfer for their interest and many useful discussions.

## REFERENCES

- [1] H. Schlarb, "Design and performance of the TESLA Test Facility collimation system," AIP Conf. Proc. **693** (2004) 209, EPAC'02, Paris, June 2002.
- [2] H. Schlarb, "Simulation of dark current transport through the TESLA Test Facility linac," DESY-M-02-01ZG, EPAC'02, Paris, June 2002.
- [3] The BESSY Soft X-ray Free Electron Laser, TDR BESSY March 2004, eds.: D. Krämer, E. Jaeschke, W. Eberhardt, ISBN 3-9809534-0-8, BESSY, Berlin (2004).
- [4] T. Bizen, T. Tanaka, Y. Asano, D. E. Kim, J. S. Bak, H. S. Lee and H. Kitamura, "Demagnetization of undulator magnets irradiated high energy electrons," Nucl. Instrum. Meth. A **467** (2001) 185.
- [5] D. R. Walz, A. McFarlane, E. Lewandowski and J. Zabdyr, "Momentum slits, collimators and masks in the SLC," PAC 1989, Chicago, Ill., March 1989.
- [6] V. Balandin, K. Flottmann, N. Golubeva and M. Korfer, "Studies of the collimator system for the TTF phase 2," DESY-TESLA-2003-17.
- [7] M. Borland, "elegant: a flexible SDDS-compliant code for accelerator simulations," Advanced Photon Source LS-287.
- [8] NLC Zeroth Order Design Report, 1996.